ELSEVIER

Polymer Vol. 37 No. 2, pp. 297–304, 1996

0032-3861/96/$15.00+0.00

Concentration profile near the surface of polymer mixtures: a Monte Carlo study

Y. Rouault*, B. Dünweg, J. Baschnagel† and K. Binder
Institut für Physik, Johannes Gutenberg-Universität Mainz, Staudinger Weg 7, D-55099 Mainz, Germany
(Received 15 May 1995; revised 29 June 1995)

The concentration profile of a symmetrical binary (AB) polymer mixture confined between two 'neutral' repulsive walls is studied by Monte Carlo simulation of the bond fluctuation model, using a chain length $N = N_A = N_B = 32$ and a distance of $D = 20$ lattice spacings between the walls. Choosing volume fractions and temperatures such that one stays inside the coexistence curve, one has A-rich and B-rich domains coexisting with each other, in each kind of domain the minority component being enriched at the surface. In contrast to simple Ising lattice gas models of mixtures, the steepest gradient in the volume fraction profile does not occur right at the surface, but a few layers away from the wall. Possible reasons for the observed flatness of this concentration profile near walls (which agrees with recent experimental findings) are briefly discussed.

(Keywords: concentration profile; polymer mixture; Monte Carlo study)

INTRODUCTION AND THEORETICAL BACKGROUND

There has been much recent interest in thin polymeric films and in surface properties of polymeric materials[1–6]: The interfacial properties of polymers in this confined geometry are important for some applications, and also pose challenging problems to their theoretical understanding.

Since many of these systems are two-component or multicomponent mixtures – which in their bulk state are typically unmixed since polymers are often not easily miscible – with large molecular weight[7–9], the surface properties of partially incompatible polymer blends are of interest. Owing to preferential attraction of one component by the wall, the surface enrichment of one component is expected[10–21] and wetting layers[10,11,16] may even form. However, even if the surface is perfectly 'neutral' (i.e. no energy preference for monomers of one kind), the symmetry between A and B is already broken due to unmixing when phase separation has taken place: then entropic reasons lead to an enrichment of the minority species at the wall[22] (i.e. entropy of mixing is more effective near the wall than it is in the bulk).

Such neutral wall effects are, in fact, well known for order–disorder phase transitions in solids, and have been studied for a long time[22–26]. Particular attention has been paid, however, only to the regime near the critical point, where it is predicted that the order parameter m_1 at the surface vanishes with a different exponent (β_1) than the order parameter m_b in the bulk (β). From the universality principle of second-order phase transitions[27] one can immediately conclude that this behaviour should then also hold at the neutral surface of a polymer mixture, i.e. the volume fraction of the majority component ϕ_A should behave as follows:

$$m_1 \equiv (\phi_{A,1} - \phi_A^{crit})/\phi_A^{crit} \propto (1 - T/T_{cb})^{\beta_1}, T \to T_{cb} \quad (1)$$

where T_{cb} is the critical temperature of unmixing in the bulk and ϕ_A^{crit} the associated volume fraction; the index 1 stands for the 'first layer' adjacent to the wall (or free surface). Equation (1) is of the same form as the order parameter in the bulk:

$$m_b \equiv (\phi_{A,rich}^{crit} - \phi_A^{crit})/\phi_A^{crit} \propto (1 - T/T_{cb})^{\beta}, T \to T_{cb} \quad (2)$$

but since $\beta_1 > \beta$ it follows that near T_c we have $m_1 < m_b$, i.e. the B-component is enriched at the surface. According to mean-field theory (applicable to polymers with very large degrees of polymerization[8,9]) one has[22–24] $\beta_1 = 1$, $\beta = 1/2$, while the Ising model universality class[27] (applicable to polymers with degrees of polymerization that are not too great[8,9]) yields[22,26] $\beta_1 \approx 0.78$, $\beta \approx 0.325$, and thus this minority enrichment is always relatively large in the critical region.

Here we are concerned with the range of this enrichment effect and the detailed shape of the enrichment profile $m(z) \equiv (\phi_A(z) - \phi_A^{crit})/\phi_A^{crit}$, as a function of distance z from the wall. In small-molecule systems, the profile is reasonably well approximated by a simple exponential decay[22]:

$$m_b - m(z) \propto \exp(-z/\xi_b) \quad (3)$$

ξ_b being the correlation length of order parameter fluctuations in the bulk. Strictly speaking, close to T_{cb}, where ξ_b is large, there is a regime $z \ll \xi_b$ where

* Permanent address: INRA Versailles, Science du Sol, Route de Saint-Cyr, F-78026, Versailles, France
† To whom correspondence should be addressed

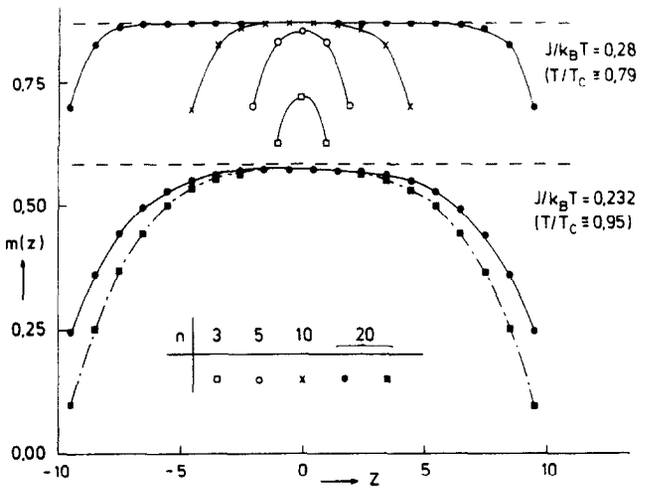

Figure 1 Local order parameter $m(z)$ plotted against distance z for films of various thicknesses na (n being the number of layers and a the lattice spacing), for the simple cubic Ising lattice model of a binary mixture AB, with nearest neighbour interaction $J = [\epsilon_{ab} - (\epsilon_{AA} + \epsilon_{BB})/2]/4$, shown at two temperatures. Broken draught lines indicate estimates for the corresponding bulk order parameter m_b. Note that the origin $z = 0$ here is chosen in the centre of the films, so the surfaces have coordinates $z = \pm(n-1)a/2$, respectively. For the 20-layer film at a normalized inverse temperature $J/k_BT = 0.232$, a case is included where the interaction parameter in the surface planes is reduced to one half of its value in the bulk (dash-dot curves) From ref. 25

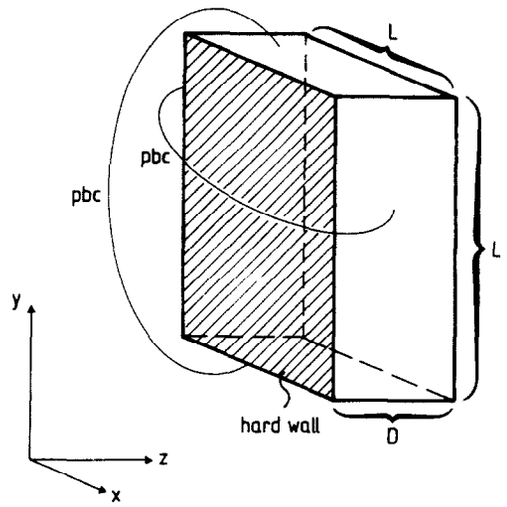

Figure 2 Sketch of the geometry of the simulation box. Two hard (impenetrable but 'neutral') walls of area $L \times L$ a distance D apart confine the two kinds of polymer chains (A,B). In the x and y directions parallel to the walls, periodic boundary conditions (pbc) are applied

equation (3) is not accurate, but it remains true that the slope $dm(z)/dz$ is largest at the surface and decreases monotonically when one moves into the bulk; see *Figure 1* for a numerical example[25]. It is evident that away from T_c, where ξ_b is of the order of the interatomic distance, the surface enrichment is restricted to one or two atomic layers near the surface only.

In polymer mixtures, on the other hand, more interesting phenomena are to be expected even away from T_{cb}, since the correlation length ξ_b is at least of the order of the gyration radius of the polymer[8,9,28]. Experimental techniques are available to measure the order parameter profile $m(z)$ near the surfaces of polymer mixtures[2,3,12-15], and interesting behaviour is found[12-15,29] that is often not in good agreement with simple mean-field-type theories[11] (one extends the Flory–Huggins description[7] of the polymer mixture in the bulk by gradient terms[10,11,28] to handle the inhomogeneous order parameter profile near the surface).

It is therefore interesting to study this problem by computer simulation, and this is the aim of the present work. Previous studies have either considered fully compatible mixtures[30] or very short chains (e.g. $N = 10$) in the presence of very strong preferential surface attraction of one species[19,20], and could not address the problem sketched above.

In the following sections we briefly describe the model and the simulation technique, and recall what is known about the phase diagram both in the bulk[31-33] and in thin-film geometry[34]. We present our simulation results for a thin-film thickness of $D = 20$ lattice spacings, restricting attention to a symmetrical polymer mixture with $N_A = N_B = N = 32$ effective bonds. Since this simulation is computationally very demanding, in order to reach the necessary statistical accuracy on $m(z)$, the variation of D and N has not been attempted here, although it would be desirable. We then briefly summarize our conclusions and present a tentative comparison with recent experimental findings[29].

MODEL AND SIMULATION METHODS

We are interested here in surface properties of both 'semi-infinite'[22] bulk systems and of thin films of thickness D but infinite (i.e. macroscopically large) in the remaining directions. Now computer simulations can deal only with systems that are finite in all their linear dimensions. Hence we choose $L \times L \times D$ geometry on the simple cubic lattice, with two repulsive walls at $z = 0$ and $z = 20$ (all lengths will be measured in units of the lattice spacing), and use periodic boundary conditions in the x and y directions (*Figure 2*). Even then, the finiteness of L is a serious problem, in particular near the critical point[5]. We thus have chosen two values of L, $L = 48$ and $L = 80$, and verify that finite size effects are negligible for the temperatures that are analysed.

As in previous work on symmetrical polymer mixtures in the bulk[31,32], we use the bond fluctuation model[36-38] to represent the polymer chains. Each chain consists of N 'effective monomers' connected by 'effective bonds'. Each effective monomer blocks all eight sites of an elementary cube from further occupation. The effective bonds are chosen from a set of bond vectors, which include (2 0 0), (2 1 0), (2 1 1), (2 2 1), (3 0 0) and (3 1 0), in addition to all permutations and sign combinations of the coordinates of these vectors. We use a volume fraction $\phi_v = 0.5$ of vacant sites, since various criteria show that the corresponding monomer density already corresponds to a dense melt[38], but on the other hand the acceptance rates for the moves of our dynamic Monte Carlo algorithm[39] are not too small. These moves are a mixture of random hopping of single monomers by one lattice unit[36-38] and 'slithering snake' type[39-42] moves. Although this dynamics is unphysical, it is preferable for the investigation of static properties since the configurations of the polymer system decorrelate significantly faster than when using the random hopping dynamics only[42].

Only a single chain length $N = 32$ is studied, owing to the high demands in computer resources for this study. When comparing this choice to experiment, one should recall that we use a coarse-grained model which can be thought of as the result of integrating $\nu = 3$–6 successive chemical bonds along the backbone of a real polymer chain into one effective bond of the model[43–45]. Thus the model corresponds to a degree of polymerization N_p in the range of about $N_p \approx 100$ to 200. The study of longer chains clearly would be desirable, but is not attempted here because then the linear dimensions D and L would both have to be much larger as well (here we use $D = 20$ and $L = 48$ to 80 throughout); note that for $N = 32$ the gyration radius of a chain is about seven lattice spacings and the end-to-end distance about 17 lattice spacings. Thus, D is just large enough not to squeeze the configuration of single chains. For $L = 48$, we have 46 080 lattice sites, i.e. 2880 monomers or 90 chains; for $L = 80$, we have 128 000 lattice sites, 8000 monomers or 250 chains in the simulation box (remember that each effective monomer blocks eight sites and only one half of the sites are occupied). Obviously, it does not make sense to study collective phenomena in polymer blends with systems containing significantly less than 10^2 chains.

As in previous work[31–34,37] we choose a square well type potential between monomers in its most symmetric form, i.e. pairwise interactions:

$$\epsilon_{AB} = -\epsilon_{AA} = -\epsilon_{BB} \equiv \epsilon \tag{4}$$

with an interaction range $\sqrt{6}$. The motivation for this choice is that then all neighbours within the first peak of the radial density distribution function contribute to these interactions[37]. We do not assume any change of these interactions near the walls (of course, the walls do have the effect that neighbours of monomers close to the wall, i.e. within the interaction range, are 'missing').

As usual[31,32,46,47] we work in the semi-grand canonical ensemble of the polymer mixture, i.e. the independent control parameters of the system are the temperature T and the chemical potential difference $\Delta\mu = \mu_A - \mu_B$ between A and B monomers. While the total number $n = n_A + n_B$ of chains is held fixed, the individual numbers of A chains (n_A) and of B chains (n_B) are not fixed, and can fluctuate. Recording their numbers and taking suitable averages one finds the average volume fractions ϕ_A, ϕ_B of A(B) monomers, respectively, as well as the average order parameter $\bar{m}$ of the system:

$$\phi_A = \tfrac{1}{2}(1 + \bar{m})(1 - \phi_v), \quad \phi_B = \tfrac{1}{2}(1 - \bar{m})(1 - \phi_v) \tag{5}$$

$$\bar{m} = \langle |n_A - n_B| \rangle / n = (\phi_A - \phi_B)/(\phi_a + \phi_b) \tag{6}$$

In addition to the moves mentioned above that are required to relax the chain configurations, one then also needs moves where A chains are transformed into B chains at fixed configuration (or vice versa)[31,32,46,47]. As we are mostly interested in the behaviour of partially incompatible systems, we study the behaviour at the coexistence curve (see below). Because of the symmetry of our model against interchange of A and B (which holds also for 'neutral' walls which do not energetically prefer one component), the coexistence curve between unmixed A-rich and B-rich phases occurs for $\Delta\mu = 0$, and hence only this value of chemical potential difference is used in the present simulations.

Equations (5) and (6) can be readily carried over to study the order parameter profile: we simply average in each plane $z = 1, \ldots, D-1$ the total density $\rho(z)$ of occupied sites as well as the individual densities $\rho_A(z)$, $\rho_B(z)$ and define:

$$m(z) = \langle |\rho_A(z) - \rho_B(z)| \rangle / \rho(z)$$
$$\rho(z) = \langle \rho_A(z) + \rho_B(z) \rangle \tag{7}$$

Note that $\rho(z)$ shows characteristic oscillations for $z \to 0$ and $z \to D$, reflecting the typical response function due to the packing constraints for hard particles near a hard wall[19,20,48–54]. In order to separate this effect from the enrichment of one species at the wall, we have found it useful to normalize $m(z)$ with $\rho(z)$ rather than with the overall density, as done for the average order parameter. Of course, due to the conservation of the total number of monomers we have the sum rule:

$$\frac{1}{D}\sum \rho(z) = 1 - \phi_v \tag{8}$$

PHASE DIAGRAMS AND GENERAL CONSIDERATIONS

Figure 3 shows the phase diagram of our model, as obtained[34] in a finite-size scaling analysis[31,32,35] for a wide range of film thicknesses D. One recognizes that in the thin-film geometry the critical temperature $T_c(D)$ is significantly depressed in comparison with the bulk critical temperature T_{cb}; in particular[31–34]:

$$k_B T_{cb}/\epsilon \cong 70.18$$
$$k_B T_c(D = 20)/\epsilon = 58.5 \pm 0.6 \tag{9}$$

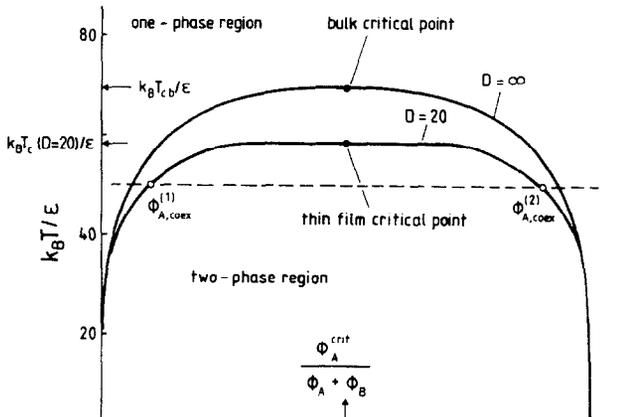

Figure 3 Phase diagram of the symmetrical polymer blend with chain lengths $N_A = N_B = N = 32$ and interactions defined in equation (4), in the plane of variables k_BT/ϵ (reduced temperature) and normalized volume fraction $\phi_A/(\phi_A + \phi_B)$ of the A monomers. The two curves show the coexistence curve for a bulk mixture ($D = 20$) and for a mixture in thin film geometry with thickness $D = 20$. Inside each curve the system does not exist as a homogeneous phase in thermal equilibrium, but is a mixture of macroscopic regions of two phases, whose volume fractions are given by the two branches of these coexistence curves (to the left and to the right of the critical points marked by dots, which occur at $\phi_A^{crit}/(\phi_A + \phi_B) = 0.5$ due to the symmetry of the model). Above the existence curve, the system is macroscopically homogeneous (notwithstanding microscopic inhomogeneities due to the enrichment layers of the respective minority components at the walls). From ref. 34 in changed form

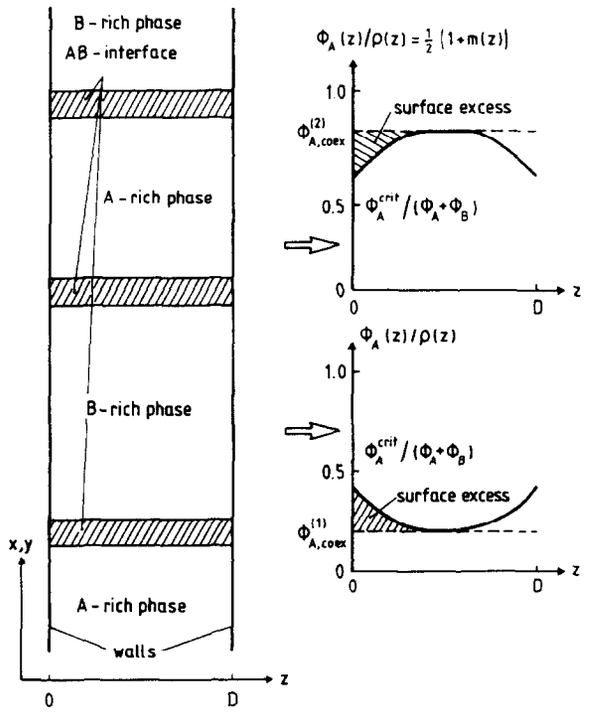

Figure 4 Schematic description of the state of a thin film of thickness D at an average volume fraction ϕ_A such that $\bar{\phi}^{(1)}_{A,coex} < \phi_A < \bar{\phi}^{(2)}_{A,coex}$ (cf. *Figure 3*). Here, $\bar{\phi}^{(1)}_{A,coex}$, $\bar{\phi}^{(2)}_{A,coex}$ are the volume fractions at the branches of the coexistence curve for the thin film, while $\phi^{(1)}_{A,coex}$ and $\phi^{(2)}_{A,coex}$ denote the branches of the coexistence curve in the limit of bulk samples, $D \to \infty$. We then expect domains of the A-rich phase (which has the volume fraction $\phi^{(2)}_{A,coex}$) and the B-rich phase (volume fraction $\phi^{(1)}_{A,rich}$) to be separated by AB interfaces that run across the film. The linear dimensions of these domains in thermal equilibrium are macroscopic, such that both the volume fraction taken by interfaces and their relative contribution to the total free energy of the system is negligibly small. The profile of the volume fraction $\phi_A(z)$, which is simply related to $m(z)$ (equation (7)) via $\phi_A(z) = \frac{1}{2}[1 - m(z)]\rho(z)$, is shown schematically both for the A-rich and the B-rich phase. Note that in our symmetric model these profiles are simply mirror images of each other along the line $\phi^{(2)}_A/\rho(z) = \phi^{crit}_A/(\phi_A + \phi_B) = 0.5$. For thick films these profiles reach the bulk coexistence values $\phi^{(1)}_{A,coex}$, $\phi^{(2)}_{A,coex}$ in the centre of the film. Shaded areas denote the surface excess concentrations discussed in the text

Near $k_B T_c(D)/\epsilon$ simulations of finite lattices are strongly affected by finite size effects. For this reason we can study with films of thickness $D = 20$ the properties of semi-infinite systems only at temperatures which are well below $T_c(D = 20)$. This strong depression of the critical temperature in thin films is due to the 'missing neighbours' at the surfaces, and the fact that in quasi-two-dimensional systems statistical fluctuations are stronger than in three-dimensional ones, and lead to a flattening of the coexistence curve[34] (the shape of the coexistence curve near T_c is controlled by a crossover[34] from the exponent $\beta \approx 0.325$ of the universality class of the three-dimensional Ising model[27] to the exponent $\beta = 1/8$ of the universality class of the two-dimensional Ising model[22]). Thus, in thin-film geometry binary blends are more miscible than in the bulk. However, we are here exclusively concerned with (partially) unmixed phases, i.e. systems that are either right at the coexistence curve or inside it. In the latter case, we have a macroscopic mixture of A-rich and B-rich domains in the thin film, as indicated schematically in *Figure 4*. Denoting the volume fractions at the B-rich (A-rich) branch of the coexistence curve *in the thin film* as $\bar{\phi}^{(1)}_{A,coex}$, $\bar{\phi}^{(2)}_{A,coex}$, the volume fraction of the A-rich domains X is given by the lever rule:

$$X = \left(\phi_A - \bar{\phi}^{(1)}_{A,coex}\right)/\left(\bar{\phi}^{(2)}_{A,coex} - \bar{\phi}^{(1)}_{A,coex}\right) \tag{10}$$

The linear dimensions of the A-rich and B-rich domains in the x, y directions should then scale like $\sqrt{X}:\sqrt{1-X}$. Note that ideally there should be only two domains separated by a single interface, since this state represents the absolute minimum of interfacial free energy contributions, but in a real system we expect that due to the slowness of polymer diffusion a multidomain configuration will be present, even after careful annealing.

Since for thick films we expect that $\phi_A(z)$ will reach the value $\phi^{(1)}_{A,coex}$ (or $\phi^{(2)}_{A,coex}$) in the centre of the film, it makes sense to define surface excess concentrations as follows[22] (for our discrete model, integrals are understood as summations, of course):

$$\phi_A^{S(B)} \equiv \lim_{D\to\infty} \int_0^{D/2} dz\{\phi_A(z) - \phi^{(1)}_{A,coex}\} \text{ B-rich phase} \tag{11}$$

$$\phi_A^{S(A)} \equiv \lim_{D\to\infty} \int_0^{D/2} dz\{\phi_A(z) - \phi^{(2)}_{A,coex}\} \text{ A-rich phase.} \tag{12}$$

For neutral surfaces we expect that $\phi_A^{S(B)}$ is positive while $\phi_A^{S(A)}$ is negative.

In our symmetric model we obviously have the symmetry relation

$$\phi_A^{S(A)} = -\phi_A^{S(B)} \tag{13}$$

but this relation is not expected to hold in real systems lacking any particular symmetries between A and B and then the two profiles shown in *Figure 4* must be studied separately.

Since the average volume fraction in the thin film is simply an integral over the profile:

$$\bar{\phi}_A = \frac{1}{D}\int_0^D \phi_A(z)dz \tag{14}$$

we have the well known relations[22]:

$$\bar{\phi}^{(2)}_{A,coex} = \phi^{(2)}_{A,coex} + \frac{2}{D}\phi_A^{S(A)} \tag{15}$$

for the A-rich phase, and

$$\bar{\phi}^{(1)}_{A,coex} = \phi^{(1)}_{A,coex} + \frac{2}{D}\phi_A^{S(B)} \tag{16}$$

for the B-rich phase. Thus an analysis of the coexistence curves for different thicknesses D (*Figure 3*) immediately yields information on these surface excess concentrations. We emphasize again that this enrichment (depletion) of A in the B-rich (A-rich) phase at the walls has nothing to do with a preferential attraction of a species by the wall, but is a purely entropic effect.

NUMERICAL RESULTS FOR THE ORDER PARAMETER PROFILES

Figure 5 shows the order parameter profiles $m(z)$ for the four temperatures $k_B T/\epsilon = 40$, 45.45, 50 and 55.56. Owing to the symmetry against interchange of both walls, which are perfectly equivalent, the profiles must be

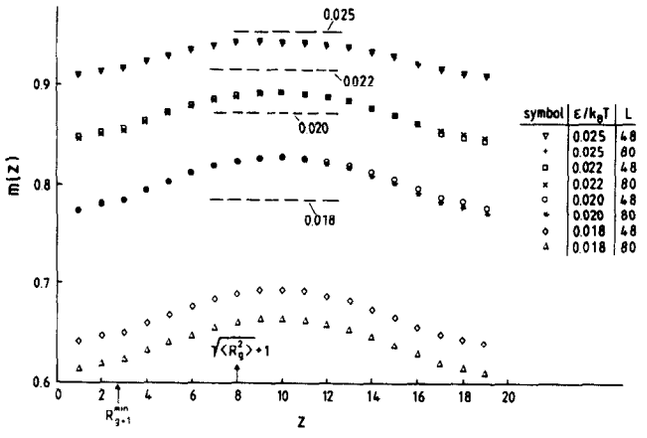

Figure 5 Order parameter profiles $m(z)$ *versus* z shown at four different temperatures. In each case two choices of the linear dimension are shown. While for $\epsilon/k_BT \geq 0.02$ between $L = 48$ and $L = 80$ are small and only due to statistical errors (which typically are estimated to be of the size of the symbols), data for $\epsilon/k_BT = 0.018$, $L = 48$ clearly suffer from finite size effects. Broken straight lines indicate the values of the bulk order parameter m_b in each case[33]. Arrows show the gyration radius and its smallest component in the eigencoordinate system of the gyration tensor[33]

symmetric around their centre ($z = 10$). Slight deviations from symmetry are at most of the size of our statistical errors, which are about the size of the symbols.

At the three lower temperatures both choices for L yield results that nicely coincide with each other, indicating that finite size effects associated with the finiteness of the linear dimension parallel to the wall are still negligible. This is gratifying, since the temperature $k_BT/\epsilon = 50$ is only about 14.5% below the critical temperature $k_BT_c(D)/\epsilon$ (equation (9)). Of course, if we move still closer ($k_BT/\epsilon = 55.56$ is about 5% below $k_BT_c(D)/\epsilon$), we do see pronounced finite size effects. However, experience with other analyses[31–34] suggests that even in this case the data for $L = 80$ should be close to the limiting behaviour for $L \to \infty$ already.

When we compare the profiles in *Figure 5* with those obtained for lattice gas models (*Figure 1*), we note a pronounced difference in the shape of these profiles. While in the Ising case the profile has its maximal slope always in the first layer right near the wall, this is obviously not true in the polymer mixture, rather we observe a region of several layers at the surfaces where the profile is very flat. Note that this region is distinctly smaller than the gyration radius $\langle R_g^2\rangle^{1/2}$ of the polymer chains in the bulk; rather this quantity (in the temperature region distinctly below T_c studied here) sets the scale on which the profile essentially reaches the value of the order parameter m_b in the bulk. However, one must remember that $\langle R_g^2\rangle^{1/2}$ is not expected to be the relevant length scale very close to the surface, due to the orientational effect of the wall on the shape of the polymer coils[48–54]. Remember that the instantaneous shape of a Gaussian polymer coil is not a sphere, but rather it is a 'flattened-egg-shaped' object, with a gyration tensor that has three distinct eigenvalues. The axes giving the eigendirections of this tensor are randomly oriented in the bulk, and then on average the coil is spherically symmetric. At the surfaces, however, best packing of the monomers is achieved if the axis corresponding to the largest eigenvalue is parallel to the wall (then the end-to-end distance of a polymer close to the wall is parallel to the wall), and the axis corresponding to the smallest eigenvalue is oriented along the z-axis perpendicular to the wall. Thus the polymer lies essentially flat on the wall, without major distortion of its internal shape (which would be very costly in terms of the entropic elastic forces of the coil). Only when we use a strong binding potential to the wall, as done in refs 19 and 20, does it become possible to get a significant distortion of the shape of such a polymer coil attached to the wall, which ultimately takes a flat pancake-like shape for very strong wall–monomer interaction[55].

From this argument we expect that the order parameter profile should be flat near the walls on the scale given by this smallest eigenvalue R_g^{min} of the gyration tensor. This quantity has recently been measured in the context of the study of AB interfaces in strongly incompatible mixtures[33] (where a similar orientational effect on coil shapes occurs), $R_g^{min} = 1.75$. This quantity is also indicated by an arrow in *Figure 5*. (Actually we show $R_g^{min} + 1$ since the first layer available for monomers is $z = 1$ rather than $z = 0$.)

The fact that R_g^{min}, obtained in a study of the interfacial structure of an AB mixture, also determines the length scale over which the $m(z)$ profile is flat, is evidence for the argument presented above that a hard wall reorients the polymers without distorting their internal structure.

We emphasize that these effects are not captured by the simple models using a Flory–Huggins-type free energy amended by gradient terms[11] and extensions thereof[16–18], since all these theories do not consider explicitly the configurational properties of the polymer coils in sufficient detail. Although at an AB interface and a hard wall coils become oriented parallel to the interface or to the surface, respectively, the profiles are quite distinct in shape near $z = 0$ in both cases. In the case of the interface the coils may cross the plane $z = 0$ for a distance of about R_g^{min} so that the B chains attached to the interface make excursions into the A-rich side of the interface and vice versa. Thus for the interfacial problem the steepest slope of the profile does occur at $z = 0$ (ref. 33), unlike *Figure 5*. As a consequence, we do not confirm the assertion of mean-field[11] theory that the profile near a wall is just a piece of the interfacial profile, cut in such a way that one satisfies suitable boundary conditions at the surface. Gratifyingly, this flattening out of concentration profiles near walls has been seen in recent experiments[29].

It is also interesting to note that for the thickness $D = 20$ (which is roughly $D \approx 3\langle R_g^2\rangle^{1/2}$) the profile even in the centre of the film falls slightly below the bulk value, for all temperatures shown. Thus bulk behaviour can be expected in polymeric films only if $D \gg \langle R_g^2\rangle^{1/2}$.

Comparing with the lattice gas problem of *Figure 1*, choosing a film thickness $D = 20$ for the polymer problem really would correspond to choosing, say, $n = 5$ for the lattice gas problem. As is evident from *Figure 1*, one can estimate m_1 (the order parameter of the first layer adjacent to the surface) rather well already even if $m(z)$ does not yet reach m_b in the centre of the films. Similar conclusions have also been drawn from other simulations studying homopolymer melts close to hard walls[56–58], which show that a change in D influences the shape of the profiles of various quantities (other

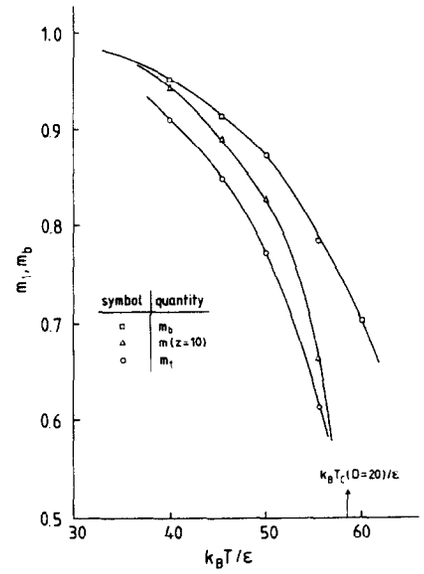

Figure 6 Plot of the local order parameter at the surface m_1 ($\equiv m(z=1)$), the local order parameter in the centre of the film ($m(z=10)$) and the order parameter of bulk systems[33] (m_b) *versus* reduced temperature. Arrow shows the location of the critical temperature of the film

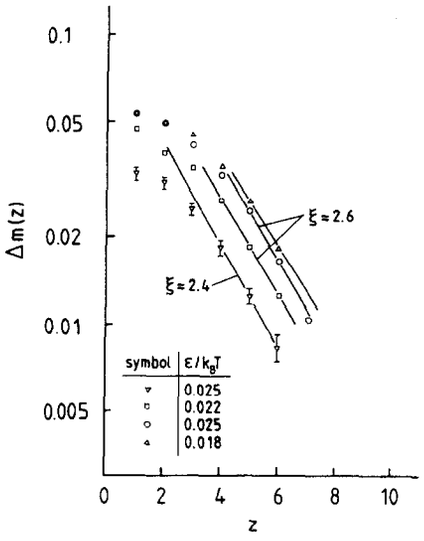

Figure 7 Semi-log plot of the deviation of the order parameter from its value in the centre of the film, $\Delta m(z) \equiv m(z=10) - m(z)$, plotted *versus* z. Straight lines indicate rough estimates of the decay constant ξ

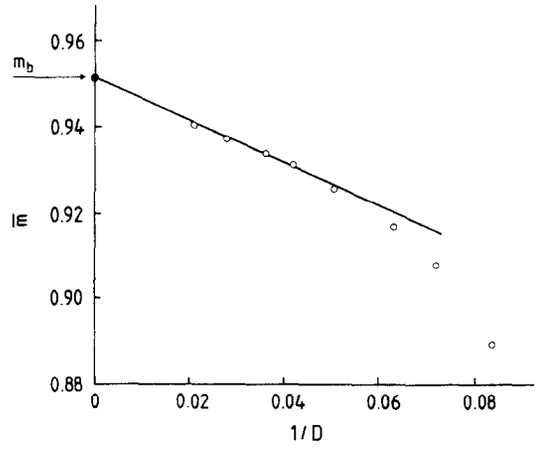

Figure 8 Plot of $\bar{m}(D)$ at $T = 40$ *versus* D^{-1}. The arrow shows m_b, as calculated in ref. 33. The slope of the straight line for $D^{-1} \to 0$ yields the order parameter excess m_s

than m) in the middle of the film, but not close to the wall. *Figure 6* compares the temperature dependence of m_b, $m(z=10)$ and m_1. Of course, near $T = T_c(D)$, m_1 no longer resembles the surface layer order parameter of the semi-infinite system; rather m_1 and $m(z=D/2)$ then become similar again, since near $T_c(D)$ the whole profile becomes flat, the system behaves in a quasi-two-dimensional fashion, and the whole profile $m(z)$ for all z vanishes with an exponent of the two-dimensional Ising universality class:

$$m(z) \propto [1 - T/T_c(D)]^{1/8} \qquad \text{all } z,\ T \to T_c(D) \quad (17)$$

In ref. 34 this was already demonstrated for the average order parameter of the thin film, $\bar{m} = (1 - D\int_0^D \mathrm{d}z\, m(z)$, cf. equation (14).

When we study the approach of $m(z)$ against its maximum value $m(z = D/2)$, in order to test for equation (3), it is clear that only data in an intermediate regime $1 + R_g^{\min} \ll z \ll D/2$ should be used. The film thickness $D = 20$ clearly is not large enough to yield such a regime, however. In order to extract at least a rough estimate, these inequalities are relaxed to $1 + R_g^{\min} \leq z \leq D/2$, and then a regime from $4 \leq z \leq 7$ is compatible with the expected exponential decay. However, as shown in *Figure 7*, the resulting correlation length is smaller (namely $2.4 \leq \xi \leq 2.6$) than the value expected theoretically[9] for temperatures well below T_c, $\xi_b \approx (\langle R_g^2 \rangle/3)^{1/2} \approx 4$. This apparently faster decay is presumably again a consequence of the fact that we are working with relatively very thin films. Our data show that one should watch carefully for finite thickness effects if one wishes to extract bulk quantities from measurements on thin films, as is sometimes done experimentally[59].

Finally, *Figure 8* shows a test of equation (15) (which can be rewritten as $\bar{m} = m_b + (2/D)m_s$, where m_s is a corresponding 'surface excess order parameter'[22]). It is seen that this relation holds for large D, while for small D distinct deviations are noted. This was expected, of course, since *Figure 5* shows that bulk behaviour in the centre of the film is reached only at very low temperatures for $D = 20$, and for smaller values of D (*Figure 8* includes data from ref. 34 where D was varied, but the profiles have not been studied for other values of D); even more pronounced deviations from equations (15) and (16) are expected.

CONCLUDING REMARKS

In this study arguments were presented to show that at the surface of a symmetric ($N_A = N_B$) binary mixture with asymmetric composition in the bulk ($\phi_A \neq \phi_B$), a surface enrichment of the minority component occurs for purely entropic reasons, i.e. without any preferential forces attracting this component to the wall. We have investigated this phenomenon for partially incompatible mixtures, held at the coexistence curve (as explained in *Figure 4*, this treatment then describes surface effects on unmixed systems at an average concentration inside the coexistence curve as well).

A striking feature of our results is the flatness of our concentration profiles close to the walls (*Figure 5*), which contrasts with corresponding results for the lattice gas model (*Figure 1*) and with theoretical treatments of surface enrichment in polymer mixtures[11,16–18]. We interpret this result in terms of the connectivity of the

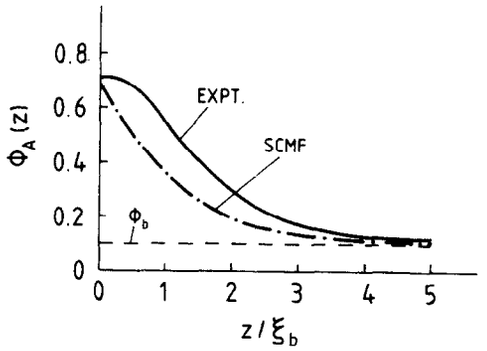

Figure 9 Comparison of an experimental surface enrichment profile (full curve) with a corresponding self-consistent meanfield calculation (dash-dot curve). Data are for a mixture of deuterated (A) and protonated (B) poly(ethylene propylene) (PEP) of degree of polymerization $N = 2250$, at $T = 70°C$ and a bulk volume fraction $\phi_b = 0.099$ of deuterated PEP. The experimental profile resulted from a neutron reflection analysis of a free surface of this mixture. After the PhD thesis of L. Norton, Cornell University, 1994, as reproduced by E. J. Kramer in ref. 29, in changed form

chains and their resistivity against elastic deformations; the closest distance that a minority chain gets to the wall is given by the smallest eigenvalue R_g^{min} of its gyration tensor, and hence on scales $z < R_g^{min}$ the profile is essentially flat. For our chain length ($N = 32$), we have[34] $R_g^{min} \approx \langle R_g^2 \rangle^{1/2}/4$, and since for many properties our model is already representative for the behaviour of very long chains[38], we assume that this result can be extrapolated to real polymers as well. In this context it is gratifying to recall that a similar behaviour has been found experimentally, simultaneously with our study and independently from it, in symmetrical mixtures of protonated and deuterated poly(ethylene propylene)[29]. *Figure 9* provides a sketch of the typical experimental results. The profile does exhibit a flat part over a distance $z \approx 0.5\xi_b$, and noting that for small bulk concentration ϕ_A the correlation length is[9] $\xi_b \approx (\langle R_g^2 \rangle/3)^{1/2}$, the distance $0.5\xi_b$ is indeed close to R_g^{min}. Of course, one should not expect that the magnitude of the surface enrichment seen in the experiment is comparable to the simulation: we deal here with a model that is 'most symmetric' in its interactions, $\epsilon_{AA} = \epsilon_{BB}$, and hence a preferential attraction to the surface resulting[60] from a term $\epsilon_{AA} - \epsilon_{BB} \neq 0$ is absent in the simulation, but presumably present in the experiment. In any case, it is gratifying that the results from our model calculation seem to be applicable to real systems. We hope that our study will stimulate additional experiments, as well as the development of a theory that describes the concentration profile more precisely. We emphasize that the concentration profile resulting from our calculation cannot be considered as a piece of a concentration profile between coexisting phases, 'cut off' by the boundary condition to enforce the surface layer concentration ϕ_1, as in mean-field theory[11]. In this interfacial problem, chains exist which have their centre of gravity right in the centre of the interface[34], and hence the position of the steepest gradient occurs (for $N_A = N_B$) exactly at the critical concentration, i.e. for order parameter $m(z) = 0$, unlike the present case where almost no chains have their centre of gravity closer to the surface than R_g^{min}.

ACKNOWLEDGEMENTS

Y. R. is grateful to INRA and J. B. to the Bundeministerium für Forschung und Technologie (BMFT; Grant Number 03M4076A3) for financial support of this work. Special thanks go to M. Müller for many helpful discussions during the various stages of this work. We are grateful to J. Klein, E. J. Kramer, T. P. Russell and U. Steiner for stimulating discussions.

REFERENCES

1 Sanchez, I. C. (Ed.) 'Physics of Polymer Surfaces and Interfaces', Butterworth-Heinmann, Boston, 1992
2 Stamm, M. *Adv. Polym. Sci.* 1992, **100**, 357
3 Tirrell, M. and Parsonage, E. E. in 'Materials Science and Technology, Vol. 12: Physical Properties of Polymeric Materials' (Ed. E. L. Thomas), VCH, Weinheim, 1993
4 Fleer, G. J., Cohen Stuart, M. A., Scheutjens, J. M. H. M., Cosgrove, T. and Vincent, B. 'Polymers at Interfaces', Chapman & Hall, London, 1993
5 Yoon, D. Y., Vacatello, M. and Smith, G. D. in 'Monte Carlo and Molecular Dynamics Simulations in Polymer Science' (Ed. K. Binder), Oxford University Press, New York, 1995, Ch. 5
6 Binder, K. *Acta Polym.* in press
7 Flory, P. J. 'Principles of Polymer Chemistry', Cornell University Press, Ithaca, 1953
8 De Gennes, P. G. 'Scaling Concepts in Polymer Physics', Cornell University Press, Ithaca, 1979
9 Binder, K. *Adv. Polym. Sci.* 1994, **112**, 181
10 Nakanishi, H. and Pincus, P. *J. Chem. Phys.* 1983, **79**, 997
11 Schmidt, I. and Binder, K. *J. Phys. (Paris)* 1985, **46**, 1631
12 Jones, R. A. L., Kramer, E. J., Rafailovich, M. H., Sokolov, J. and Schwarz, S. A. *Phys. Rev. Lett.* 1989, **62**, 280
13 Sokolov, J., Rafailovich, M. H., Jones, R. A. L. and Kramer, E. J. *Appl. Phys. Lett.* 1989, **54**, 590
14 Steiner, U., Eisen, E., Klein, J., Budkowski, A. and Fetters, L. B. *Science* 1992, **258**, 1126
15 Budkowski, A., Steiner, U. and Klein, J. *J. Chem. Phys.* 1992, **97**, 5229
16 Carmesin, I. and Noolandi, J. *Macromolecules* 1989, **22**, 1689
17 Cohen, S. M. and Muthukumar, M. *J. Chem. Phys.* 1989, **90**, 5749
18 Fredrickson, G. H. and Donley, J. P. *J. Chem. Phys.* 1992, **97**, 8911
19 Wang, J. S. and Binder, K. *J. Chem. Phys.* 1991, **94**, 8537
20 Wang, J. S. and Binder, K. *Makromol. Chem., Theory Simul.* 1992, **1**, 49
21 Tang, H., Szleifer, I. and Kumar, S. K. *J. Chem. Phys.* 1994, **100**, 5367
22 Binder, K. in 'Phase Transitions and Critical Phenomena, Vol. 8' (Eds C. Domb and M. S. Green), Academic Press, New York, 1983, p. 1
23 Binder, K. and Hohenberg, P. C. *Phys. Rev.* 1972, **6**, 3461
24 Binder, K. and Hohenberg, P. C. *Phys. Rev. B* 1974, **9**, 2194
25 Binder, K. *Thin Solid Films* 1974, **20**, 367
26 Landau, D. P. and Binder, K. *Phys. Rev. B* 1990, **41**, 4633
27 Fisher, M. E. *Rev. Mod. Phys.* 1974, **46**, 597
28 Binder, K. *J. Chem. Phys.* 1983, **79**, 6387
29 Kramer, E. J. *Faraday Discuss.* in press
30 Cifra, P., Karasz, F. E. and Macknight, W. J. *Macromolecules* 1992, **25**, 4895
31 Deutsch, H.-P. and Binder, K. *Macromolecules* 1992, **25**, 6214
32 Deutsch, H.-P. *J. Stat. Phys.* 1992, **67**, 1039
33 Müller, M., Binder, K. and Oed, W. *Faraday Trans.* in press
34 Rouault, Y., Baschnagel, J. and Binder, K. *J. Stat. Phys.* in press
35 Binder, K. and Heermann, D. W. 'Monte Carlo Simulation in Statistical Physics: An Introduction', Springer, Berlin, 1988
36 Carmesin, I. and Kremer, K. *Macromolecules* 1988, **21**, 2819
37 Deutsch, H.-P. and Binder, K. *J. Chem. Phys.* 1991, **94**, 2294
38 Paul, W., Binder, K., Heermann, D. W. and Kremer, K. *J. Phys. (Paris)* 1991, **II1**, 37
39 Kremer, K. and Binder, K. *Comp. Phys. Rep.* 1988, **7**, 259
40 Kron, A. K. *Polym. Sci. USSR* 1965, **7**, 1361
41 Wall, F. T. and Mandel, F. *J. Chem. Phys.* 1975, **63**, 4592
42 Müller, M. and Binder, K. *Computer Phys. Commun.* 1994, **84**, 173
43 Baschnagel, J., Binder, K., Paul, W., Laso, M., Suter, U. W., Batoulis, J., Jilge, W. and Bürger, T. *J. Chem. Phys.* 1991, **95**, 6014
44 Baschnagel, J., Qin, K., Paul, W. and Binder, K. *Macromolecules* 1992, **25**, 3117

45 Binder, K. *Makromol. Chem., Macromol. Symp.* 1991, **50**, 1
46 Sariban, A. and Binder, K. *J. Chem. Phys.* 1987, **86**, 5853
47 Sariban, A. and Binder, K. *Macromolecules* 1988, **21**, 711
48 Kumar, S. K., Vacatello, M. and Yoon, D. Y. *J. Chem. Phys.* 1988, **89**, 5206
49 Kumar, S. K., Vacatello, M. and Yoon, D. Y. *Macromolecules* 1990, **23**, 2189
50 Baschnagel, J. and Binder, K. preprint
51 Bitsanis, I. A. and Hadziioannou, G. *J. Chem. Phys.* 1990, **92**, 3827
52 Dickman, R. and Hall, C. K. *J. Chem. Phys.* 1988, **89**, 3168
53 Yethiraj, A. and Hall, C. K. *Macromolecules* 1990, **23**, 1865
54 Mansfield, K. F. and Theodorou, D. N. *Macromolecules* 1989, **22**, 3143
55 Eisenriegler, E., Kremer, K. and Binder, K. *J. Chem. Phys.* 1982, 77, 6296
56 Kumar, S. K., Vacatello, M. and Yoon, D. Y. *Macromolecules* 1990, **23**, 2189
57 ten Brinke, G., Ausserre, D. and Hadziioannou, G. *J. Chem. Phys.* 1989, **89**, 4374
58 Yethiraj, A. *J. Chem. Phys.* 1994, **101**, 2489
59 Budkowski, A., Steiner, U., Klein, J. and Schatz, G. *Europhys. Lett.* 1992, **18**, 705
60 Puri, S. and Binder, K. *Phys. Rev. E* 1994, **49**, 5359